Solar Energy Materials and Solar Cells 186 (2018) 259–265

Contents lists available at ScienceDirect

Solar Energy Materials and Solar Cells

journal homepage: www.elsevier.com/locate/solmat

Effect of $CdCl_2$ passivation treatment on microstructure and performance of CdSeTe/CdTe thin-film photovoltaic devices

Amit H. Munshi[a,*], Jason M. Kephart[a], Ali Abbas[b], Adam Danielson[a], Guillaume Gélinas[c,d], Jean-Nicolas Beaudry[d], Kurt L. Barth[a], John M. Walls[b], Walajabad S. Sampath[a]

[a] Department of Mechanical Engineering, Colorado State University, Fort Collins, CO 80523, USA
[b] CREST (Centre for Renewable Energy Systems Technology), Wolfson School of Mechanical, Electrical and Manufacturing Engineering, Loughborough University, Leicestershire LE11 3TU, United Kingdom
[c] Département de Génie Physique and Regroupement Québécois sur les matériaux de pointe (RQMP), École Polytechnique Montréal, Case Postale 6079, Succursale Centre-Ville, Montreal, QC, Canada H3C 3A7
[d] 5N Plus Inc., Montreal, QC, Canada H4R 2B4

ABSTRACT

The effects of the $CdCl_2$ passivation treatment on thin-film CdTe photovoltaic films and devices have been extensively studied. Recently, with an addition of CdSeTe layer at the front of the absorber layer, device conversion efficiencies in excess of 19% have been demonstrated. The effects of the $CdCl_2$ passivation treatment for devices using CdSeTe has not been studied previously. This is the first reported study of the effect of the treatment on the microstructure of the CdSeTe /CdTe absorber. The device efficiency is < 1% for the as-deposited device but this is dramatically increased by the $CdCl_2$ treatment. Using Scanning Transmission Electron Microscopy (STEM), we show that the $CdCl_2$ passivation of CdSeTe/CdTe films results in the removal of high densities of stacking faults, increase in grain size and reorientation of grains. The $CdCl_2$ treatment leads to grading of the absorber CdSeTe/CdTe films by diffusion of Se between the CdSeTe and CdTe regions. Chlorine decorates the CdSeTe and CdTe grain boundaries leading to their passivation. Direct evidence for these effects is presented using STEM and Energy Dispersive X-ray Analysis (EDX) on device cross-sections prepared using focused ion beam etching. The grading of the Se in the device is quantified using EDX line scans. The comparison of CdSeTe/CdTe device microstructure and composition before and after the $CdCl_2$ treatment provides insights into the important effects of the process and points the way to further improvements that can be made.

1. Introduction

Thin film CdTe based photovoltaics have recently demonstrated lowest cost of electricity for utility scale energy generation. The technology is recognized to be an important contributor to the global need for sustainable renewable energy. The technology is low cost and has proven industrial scalability [1]. With improvements in fabrication processes, research scale small devices with device efficiency up to 22.1% [2] have been reported while commercial module efficiencies of 18.6% [3] have been achieved. The average efficiency of commercial production modules has increased from 13.5% to 16.2% between 2014 and 2016 [4,5]. Device efficiency has been improved recently by modifying the cell architecture by introducing new materials into the buffer layer and into the absorber. These modifications have not resulted in increased manufacturing complexity or cost. The most significant improvement has involved the introduction of Se to form a CdSeTe layer at the interface with an intrinsic but fully transparent buffer layer such as magnesium doped zinc oxide (MZO). These devices have demonstrated a conversion efficiency above 19% with short-circuit current density (J_{SC}) of over 28 mA/cm^2 [6]. Devices fabricated using a CdTe-only absorber using similar fabrication conditions with efficiency 18.6% have been reported by the authors [7]. This suggests incorporation of Se is an important improvement in device fabrication technology. Optimization of the CdSeTe/CdTe absorber is required to further optimize the composition of these films and achieve improvement in device efficiency. It is important to understand the behavior of these CdSeTe/CdTe films under processing conditions. It is well known that the cadmium chloride annealing process is vital to obtain good efficiencies with conventional CdS/CdTe devices. Here we report on the effects of the treatment on the microstructure and composition of CdSeTe/CdTe devices and relate these effects to device performance using direct evidence from device cross sections investigated using Scanning Transmission Electron Microscopy (STEM) and Energy Dispersive X-ray Analysis (EDS).

* Corresponding author.

https://doi.org/10.1016/j.solmat.2018.06.016
Received 27 March 2018; Received in revised form 31 May 2018; Accepted 8 June 2018
Available online 06 July 2018
0927-0248/

In this study, two thin-film devices were deposited with CdSeTe and CdTe using sublimation under identical process conditions. One as deposited device was characterized while the second device was treated with $CdCl_2$ and then characterized. The $CdCl_2$ treatment is a critical process step in fabrication of high efficiency CdTe photovoltaic devices [8,9]. In this study cross–sections of the CdSeTe/CdTe devices, as deposited and $CdCl_2$ treated, were analyzed using cross-section scanning transmission electron microscope (STEM) imaging, energy dispersive X-ray spectroscopy (EDS) elemental mapping, EDS line scans and EDS selected area analysis. In addition, the electrical performance of these research scale small devices was obtained to correlate with the structural analyses. The analysis of these devices show similar behavior between the CdSeTe/CdTe graded absorber devices and the CdTe-only devices. Effect of $CdCl_2$ passivation treatment on grain structure of these films is thoroughly studied. The $CdCl_2$ passivation treatment also causes removal of stacking faults in CdSeTe as previously observed in CdTe films. Elemental analysis of fabricated films using cross-section TEM and EDS is used to understand the effect of $CdCl_2$ treatment on material composition of the film. Behavior of chlorine observed in CdSeTe/CdTe films with $CdCl_2$ is similar to CdTe-only films [10]. Electrical characterization of these devices shows a steep improvement in device performance after the $CdCl_2$ passivation treatment.

2. Experimental

The cells used in the study were deposited on NSG TEC 10 soda lime glass coated with fluorine-doped tin oxide (FTO) to function as a transparent conducting oxide (TCO). A 100 nm thick $Mg_xZn_{1-x}O$ (MZO) buffer layer was deposited using RF sputter deposition [11,12]. Identical CdSeTe films were sublimated on 2 TEC 10 glass substrates that were coated with MZO using an optimized deposition process followed by sublimation of the CdTe layer. On one of these substrates, $CdSe_xTe_{1-x}$ (CdSeTe) and CdTe depositions were followed by $CdCl_2$ passivation, performed in-line without breaking vacuum. The substrate was heated to ~530 °C before starting the sublimation of CdSeTe. The temperature of the substrate was measured in-situ using a pyrometer located outside the pre-heating station. The thin-films for this study were deposited using the advanced deposition system with 9 process stations at Colorado State University previously optimized for fabrication of CdTe based thin-film devices [13].

The CdSeTe composition used for this study had 40% CdSe in the source material and the as-deposited films had a band-gap of ~ 1.41 eV measured using optical transmission measurements and the Tauc plot method. The CdSeTe vapor source was heated to 575 °C while the substrate heater was maintained at 420 °C and CdSeTe films of ~ 1.5–2.0 μm thickness were deposited. After deposition of CdSeTe, the substrate was moved to the CdTe sublimation vapor source and a film ~3.5 μm thick was deposited. The total thickness of CdSeTe and CdTe film stack was measured to be ~5 μm using a profilometer. The CdTe sublimation source temperature was maintained at 555 °C and the substrate heater for this source was maintained at 500 °C. One of the substrates was moved to the $CdCl_2$ vapor passivation treatment station in-situ without breaking vacuum after the CdTe film deposition. The $CdCl_2$ sublimation source was maintained at 447 °C while the substrate heater for this source was heated to 430 °C. The $CdCl_2$ passivation treatment was performed for 600 s. These temperatures were determined after several experimental iterations to optimize the $CdCl_2$ treatment such that at the end of the 600 s treatment there was a thin film of $CdCl_2$ deposited on the substrate. Following the $CdCl_2$ passivation treatment, the substrate was moved to a cooling station without any active heating and allowed to cool for 180 s. No post $CdCl_2$ treatment annealing was performed during this experiment. After this process step, the substrate was removed from the vacuum chamber and the residual $CdCl_2$ film was rinsed using de-ionized water.

Thereafter, the films were heated to ~ 140 °C, and CuCl was deposited on the film surface for 110 s. This was followed by 220 s of annealing at 220 °C, both in vacuum, to form a Cu doped back contact. A ~ 30-nm Te film was evaporated to improve the back-contact [14]. After the deposition of Te, the substrates were cut in half. One half was used for materials characterization using TEM and TEM/EDS. Carbon and nickel paint in a polymer binder was sprayed on the second half of these films to form the back electrode. These halves with carbon and nickel back electrode were masked and delineated to form 10 small scale devices with an area of ~ 0.55 cm^2, that were tested for electrical performance using current density vs voltage measurements using a 1.5 AM spectrum. ABET Technologies 10,500 solar simulator with uniform illumination accessory was used to illuminate the devices for measurements. The lamp used for illumination as ozone free DC xenon arc lamp that produces 1Sun power output over 35 mm diameter field and, met ASTM, IEC and JIS Class A AM1.5 G output requirements. Current density v/s voltage curves were generated based on electrical measurements performed using Keithley 2420 SourceMeter controlled by a LabView program. Short-circuit current density was calibrated to cells measured by NREL. Device areas were measured using a webcam that took an image of a backlit solar cell and counted the pixels below certain brightness. Both the light intensity and area were calibrated for each set of measurements. The cells were contacted by a fixture of spring loaded gold pins that provided a 4-point connection and collect current from all around the front contact of the device. The setup accurately measures the J-V parameters and the agreement of these measurements with an externally certified photovoltaic device is shown in the Supplementary section.

Specimen foils for scanning transmission electron microscopy (STEM) were prepared using an FEI focused ion beam (FIB) dual beam system using a standard in-situ lift out method [7]. STEM specimen preparation and imaging were performed at Loughborough University, U.K. STEM imaging was performed using a FEI Tecnai F20 S/TEM equipped with Gatan Bright and Dark field STEM detectors, Fischione High Angle Annular Dark Field (HAADF) STEM detector and an Oxford Instruments X-Max 80 mm^2 windowless energy-dispersive spectrometer (EDX). STEM imaging was performed at 200 kV with a camera length of 100 mm and condenser aperture size of 70 μm using a spot size of 7. Such an aperture size provides a good resolution with lower depth of field. However, the specimen being thin TEM specimen lower depth of field does not affect the image quality. HAADF images were collected in conjunction with STEM bright field images. HAADF imaging gave a unique perspective as the higher the atomic weight of the material, the more the electrons pass through the sample to be detected. Therefore the amount of signal collected depends on the atomic weights of the elements within the sample, providing atomic weight contrast in the image.

The STEM system was equipped with a Silicon Drift Detector (SDD) allowing high spatial resolution Energy Dispersive X-ray (EDX) measurements and chemical mapping. This was useful to map the diffusion of elements such as chlorine and selenium in the absorber matrix. EDX spectra were collected for 120 s. Elemental maps were collected using the largest condenser aperture (150 μm) with the largest spot size. Strength of condenser lens controls probe size and final probe current. Larger condenser aperture allows more current to pass through to become probe current on the specimen. Large condenser aperture and spot size were used to achieve high EDS output signal while maintaining lower dead time. The dead time was further controlled by changing the process time; each frame took approximately 120 s to collect. Maps were collected from 10 min up to 1 h with no discernible sample drift.

3. Characterization

Cross-sections of as deposited CdSeTe/CdTe films and devices following the $CdCl_2$ passivation treatment were imaged using STEM (Fig. 1). Fig. 1A shows the grain structure of an as deposited CdSeTe/CdTe absorber layer. Large number of small grains can be observed near the CdSeTe/CdTe and MZO interfaces. In the as-deposited film, the

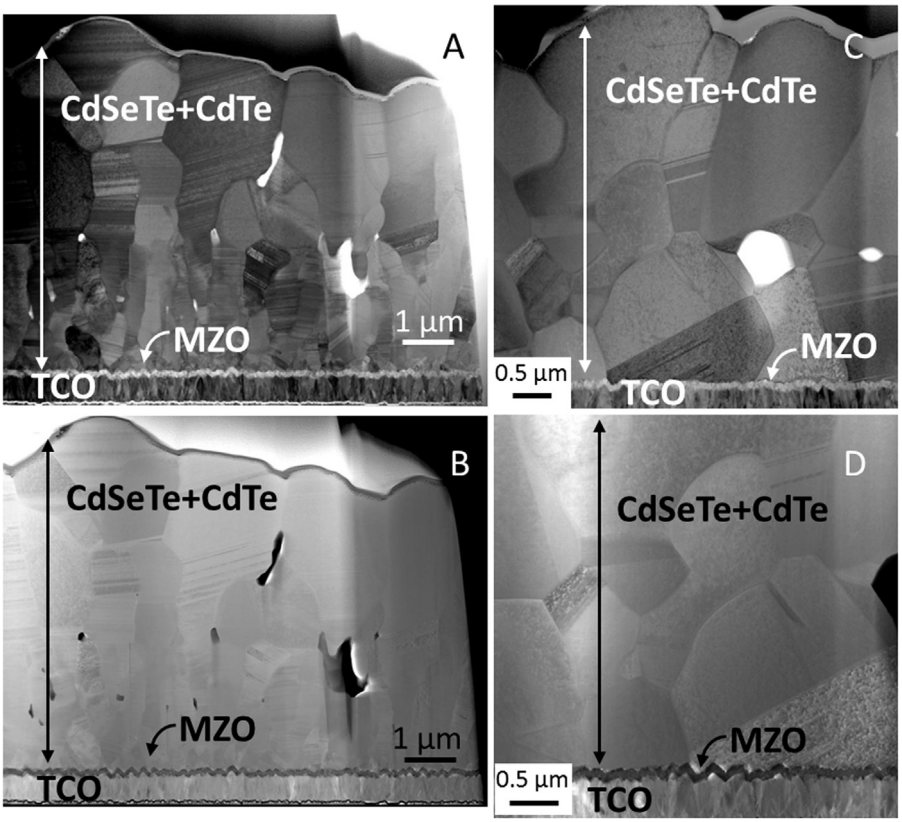

Fig. 1. (A) Cross-section bright field image of as deposited CdSeTe/CdTe film (B) Cross-section dark field image of as deposited CdSeTe/CdTe film (C) Cross section bright field image of CdSeTe/CdTe film after $CdCl_2$ passivation (D) Cross section dark field image of CdSeTe/CdTe film after $CdCl_2$ passivation.

CdSeTe grains are small at the CdSeTe/MZO interface, and grow progressively larger as the distance from the interface increases. It is also notable that before $CdCl_2$ passivation treatment, the grains contain a high density of stacking faults [15]. Numerous voids are observed between the grains. There are no voids visible at the interface of the CdSeTe/CdTe absorber and the MZO buffer layer. In addition, no voids or physical degradation of MZO film is observed before or after $CdCl_2$ passivation treatment. The MZO is a continuous film conformal to the underlying TCO layer. Voids in the absorber layer are more distinctly visible in the dark-field image.

Figs. 1C and 1D show cross-sections of the CdSeTe/CdTe absorber device that has been passivated using the $CdCl_2$ treatment. The bright-field image in Fig. 1C shows grain growth in the absorber film and particularly in the CdSeTe. No small grains are observed at the interface of CdSeTe/CdTe absorber and the MZO buffer layer. In addition, no stacking faults are now visible in these films, however, twin-boundaries are observed in most of the grains. Figs. 1C and 1D show that most of the voids present before passivation treatment have been removed and no voids are seen at the interface of CdSeTe/CdTe absorber and MZO buffer. From Fig. 1D it can also be observed that the MZO layer is not depleted and is conformal over the underlying TCO. The interface between the absorber and the buffer layer is abrupt with no evidence of intermixing between these layers.

To further understand the effect of the $CdCl_2$ treatment on the CdSeTe/CdTe devices, cross-section specimens were used to obtain elemental maps using energy dispersive X-ray spectroscopy (EDS). It is important to note that colors used for EDS elemental maps are arbitrary and colors themselves do not have any particular significance. Prior to the $CdCl_2$ passivation, the as deposited films have a distinct CdSeTe layer as shown in Fig. 2A as can be observed from Se as well as Te elemental maps. Distinct layers of CdSeTe and CdTe are observed with no evidence of diffusion between these layers during the deposition process. After the $CdCl_2$ treatment, observing Se elemental map the film shows grading of the CdSeTe into the CdTe layer (Fig. 2b). No distinct interface exists between the CdSeTe and CdTe after $CdCl_2$ treatment. It should be noted that the strong Selenium signal found at the top of the Se maps in Figs. 2A and 2B is in actuality the signal from platinum, only applied to the samples during TEM sample preparation. Fig. 2C shows the graded region of the film in greater detail. While diffusion of Se into the CdTe layer is clear, the MZO layer is unaffected and remains intact. No degradation of the MZO buffer occurs during the processing of these films. Cl is observed to decorate the grain boundaries and the MZO/CdSeTe interface. No Cl within detection limits of EDS is observed at the MZO/TCO interface; however, some Cl does appear to diffuse between the MZO grains. The TCO acts as a barrier to the further diffusion of Chlorine.

For a detailed understanding of diffusion profiles of the CdSeTe and CdTe films, EDS line scans were performed and these are shown in Fig. 3. Se is clearly observed to replace Te in the film while Cd remains unaffected. In Fig. 3B, a sharp pickup in Te towards the contact at the back of the film. This is due to a thin film of Te deposited at the back surface to improve the back contact. A comparison of the Se profile in the two films confirms that the Se is diffused into the CdTe layer following the $CdCl_2$ treated film. The untreated film appears to be slightly graded and Se composition does not appear to drop abruptly as observed in the EDS elemental maps. To verify if this is an artifact of beam size and scan area, the films are further investigated in Fig. 4.

Fig. 4A supports the earlier observation from the EDS elemental map and line scans that the as deposited CdSeTe film has ~ 10% atomic composition of Se while the region scanned immediately on top of the CdSeTe film within the CdTe layer has no detectable levels of Se. This suggests that the slightly graded drop in Se content that is observed in the line scan in Fig. 3A of as deposited film is an artifact of the probing beam size and the CdSeTe film roughness. The CdSeTe is relatively rough because it has been grown on the underlying rough TCO. Fig. 4B also verifies that grading of the CdSeTe/CdTe film occurs with the

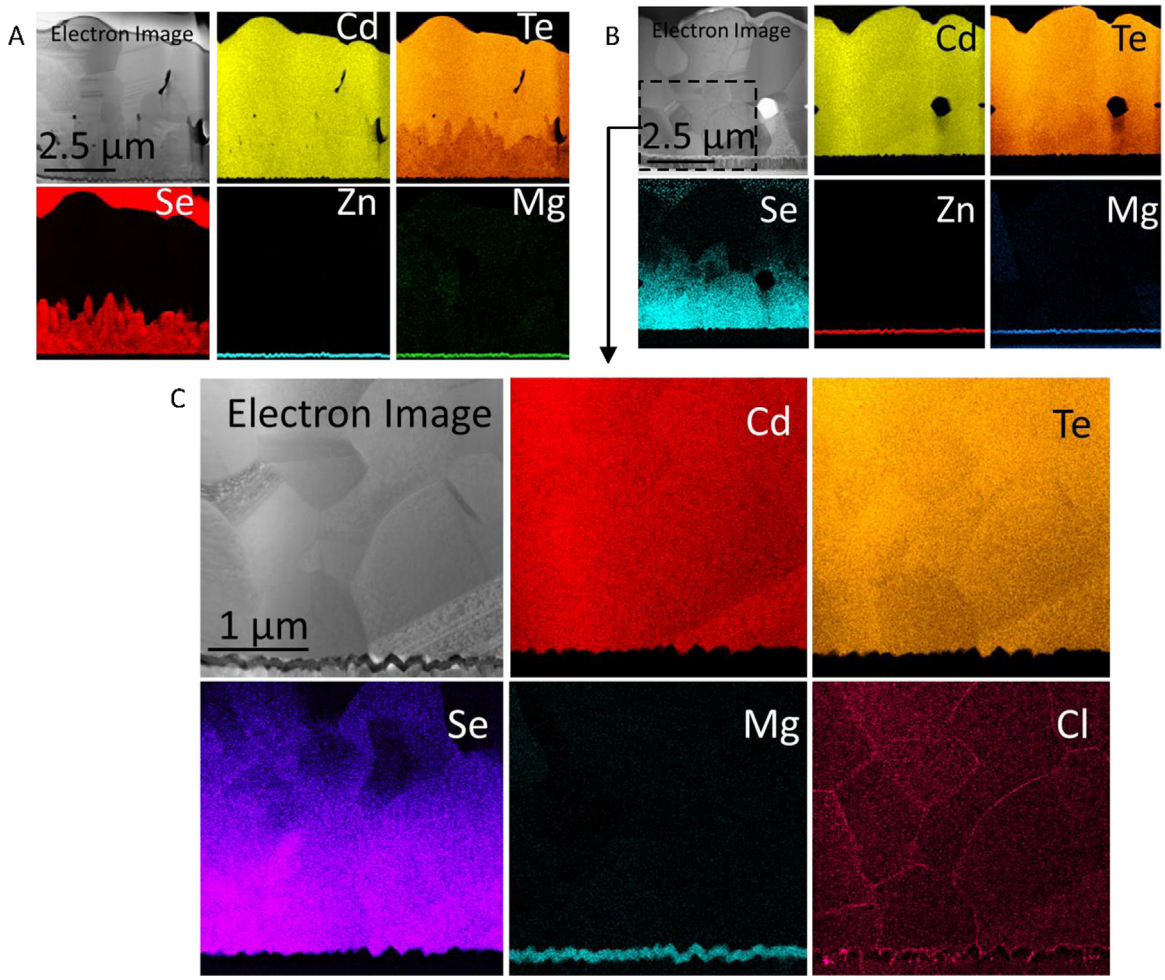

Fig. 2. (A) Cross-section STEM/EDS maps showing elemental distribution in as deposited CdSeTe/CdTe films (B) Cross-section STEM/EDS map showing elemental distribution in CdSeTe/CdTe films after $CdCl_2$ passivation treatment (C) Higher magnification elemental maps of the area rich in Se as marked in figure B.

$CdCl_2$ treatment. The 4 areas selectively scanned show the Se content reducing from 9.4% to 1.2% as the measurements are made progressively further from the MZO/CdSeTe interface.

The effect of $CdCl_2$ on the CdSeTe/CdTe film stack has been studied in detail. It was also important to correlate the effect of changes in film morphology and composition with device performance. Therefore, devices were fabricated using these two films and their performance was measured using current density vs voltage measurements. Various parameters viz. short-circuit current density (J_{SC}), open-circuit voltage (V_{OC}), fill-factor and percentage conversion efficiency were measured.

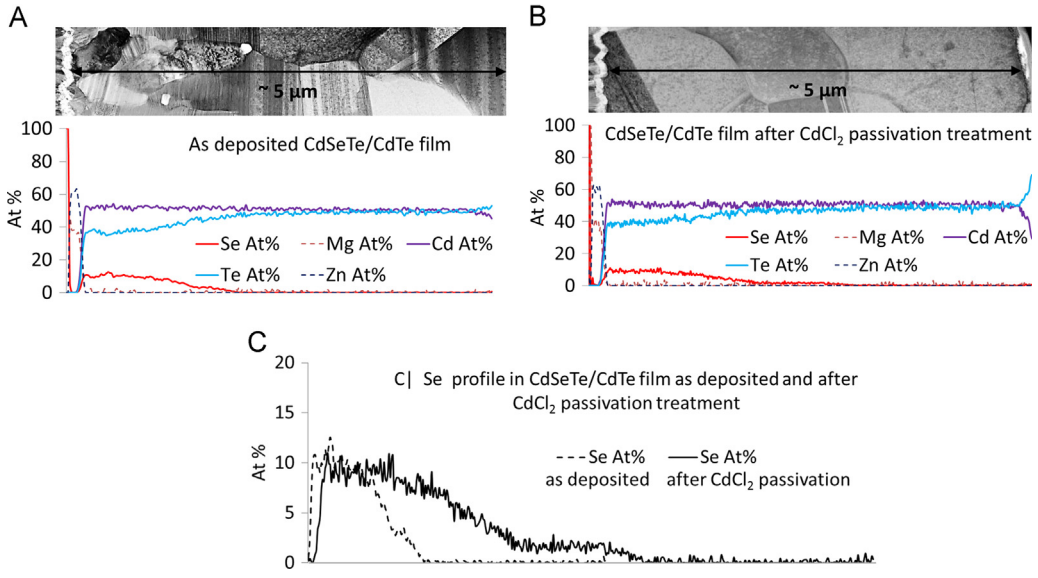

Fig. 3. (A) Cross-section STEM/EDS line scan showing elemental profile in as deposited CdSeTe/CdTe films (B) Cross-section STEM/EDS line scan showing elemental profile in CdSeTe/CdTe films after the $CdCl_2$ passivation treatment (C) Comparison of Se profile in as deposited CdSeTe/CdTe films and in films after the $CdCl_2$ passivation treatment.

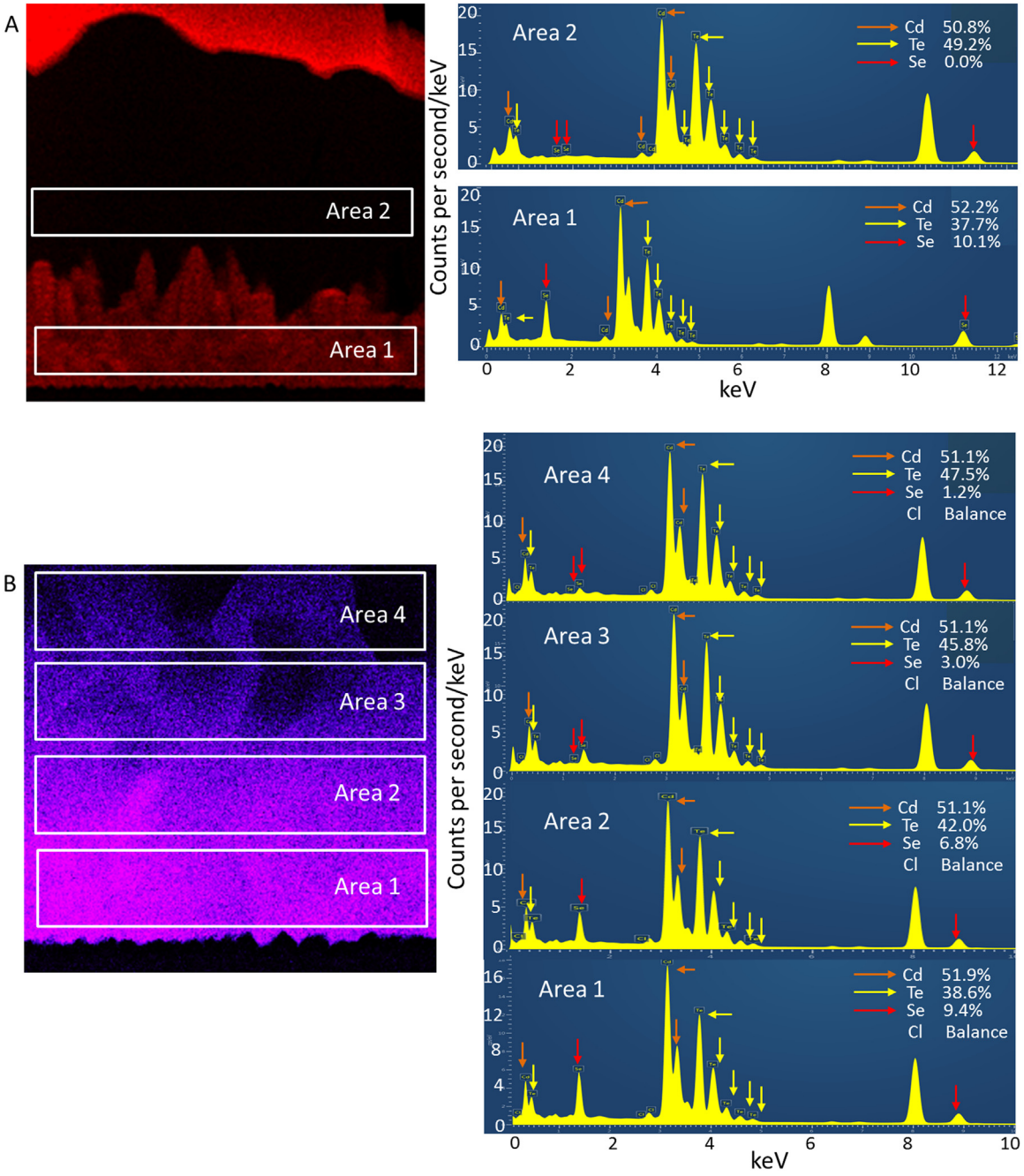

Fig. 4. (A) Selected areas scanned to determine the Se composition in the as deposited CdSeTe and CdTe films (B) Part of the film graded with Se analyzed by scanning 4 selected areas across the film.

The measurement plots are shown in Fig. 5 and comparison of J_{SC}, V_{OC}, fill-factor and conversion efficiency are summarized in Table 1. The devices were measured internally at Colorado State University using a J-V measurement system that has device measurements externally verified by a certified laboratory. The verification of accuracy of the measurements can be seen in Supplementary section.

It is clearly observed that the effect of $CdCl_2$ passivation on CdSeTe/CdTe films is extremely important for fabrication of devices with good conversion efficiency. The device efficiency improves from 0.01% to 16.8% following the $CdCl_2$ passivation treatment. A similar device with CdTe absorber treated using $CdCl_2$ was fabricated with an efficiency of 18.3% that was certified by ILX Lightwave Newport.

4. Discussion

As-deposited CdSeTe/CdTe devices and devices treated with $CdCl_2$ have been characterized to understand the effect of the $CdCl_2$ passivation treatment on the film microstructure and elemental distribution, and correlate this with electrical performance. The grain microstructure shows increase in grain size particularly for the CdSeTe layer with the $CdCl_2$ passivation treatment. We also observe the removal of stacking faults terminating at the grain boundaries. These observations are similar to those made in conventional CdTe-only films with and without $CdCl_2$ treatment [8,9,16,17]. The $CdCl_2$ treatment is known to cause recrystallization and grain growth in CdTe films [16]. The small grains of CdSeTe observed at the MZO/CdSeTe interface in the as deposited films grow into much larger grains after the $CdCl_2$ passivation

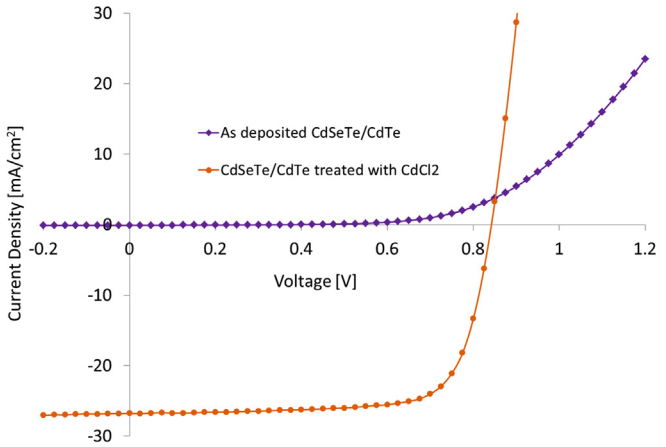

Fig. 5. Current density vs voltage showing comparison of the electrical performance of the CdSeTe/CdTe devices before and after the $CdCl_2$ passivation treatment. Please see Supplementary section to verify accuracy of these measurements.

Table 1
Summary of Electrical Performance of as Deposited CdSeTe/CdTe Device Compared to $CdCl_2$ treated device.

	Cell area (cm_2)	J_{SC} (mA/cm^2)	V_{OC} (mV)	% Fill-factor	% Efficiency
As deposited	0.553	0.1	387	34.1	0.01
$CdCl_2$ treated	0.548	26.8	842	74.5	16.8

treatment. As deposited films also contain several voids; most of which are concentrated in the CdSeTe layer and at the CdSeTe/CdTe interface. The $CdCl_2$ treatment removes most of these voids. Fewer but larger voids are observed in films treated following the $CdCl_2$ passivation. It may be possible that during the grain growth with $CdCl_2$ passivation, some of these voids agglomerate into larger voids. The effects of these voids on device performance require further investigation. The MZO buffer layer is stable during the high temperature processing and no diffusion of elements or damage to MZO layer is observed.

Elemental distribution of Cd, Se, Te, Mg, Zn and Cl have been studied in detail using EDS elemental maps, EDS line scans and EDS scans of selected areas. These results show that the CdSeTe and CdTe layers remain distinct in as deposited films and there is no or little diffusion between these layers. The $CdCl_2$ treatment acts as a very effective process to diffuse CdSeTe into the CdTe layer removing the abrupt interface between CdSeTe and CdTe. This may be critical for good device performance but diffusion of CdSeTe/CdTe without $CdCl_2$ passivation, grain growth and removal of stacking faults requires further investigation. The $CdCl_2$ passivation treatment results in grain growth in CdTe films. In addition, the $CdCl_2$ treatment is also known to promote diffusion of sulfur in CdS/CdTe devices [18]. The $CdCl_2$ treatment leads to the diffusion of Se in a similar way to form a graded absorber layer. The treatment leads to the intermixing of the two layers. It has also been reported that after $CdCl_2$ treatment, Cl accumulates at CdTe grain boundaries in CdTe-only films and presence of Cl has an electronic effect on thin-film device performance through passivation. This mechanism also occurs in CdSeTe/CdTe thin-films and devices. The Cl decorates both the CdSeTe and CdTe grain boundaries in an identical way [10]. It is also observed that small concentrations of Cl accumulate at the MZO/CdSeTe interface but not at the MZO/TCO interface. These observations are also similar to behavior of Cl after $CdCl_2$ passivation treatment in conventional CdTe-only devices. Therefore it can be assumed that Cl has similar material and electronic effects on CdTe-only and CdSeTe/CdTe films. Moreover, there is a strong indication that Se diffusion along grain boundaries as well as the grain bulk. This can have strong effect on lattice defects, band-gap, etc. at the grain boundaries and thus strong implications on device performance. These effects need to be identified and their effects characterized. Mg and Zn are known to be mobile species and tend to diffuse within the thin-films during high temperature processing. However, MZO appears to be very stable at elevated temperatures and no diffusion of Mg or Zn has been observed within the detection limits of EDS.

Measurements of device performance of as deposited CdTe-only and CdSeTe/CdTe devices compared to $CdCl_2$ treated devices are also similar. As deposited CdTe-only film have very poor performance but after $CdCl_2$ passivation there is a steep improvement in efficiency [17]. This is also observed in CdSeTe/CdTe device performance as demonstrated in this study. This is understood to be due to Cl passivating the grain boundaries and this is associated with the removal of planar defects [19]. High densities of stacking faults observed in the as deposited material are completely removed. Twin-boundaries are present in CdSeTe/CdTe films after passivation treatment, but they are low energy and benign in CdTe-only devices [15]. Since the behavior of CdSeTe/CdTe films and devices are similar to CdTe-only devices, it can be assumed that twin-boundaries do not act as recombination centers in CdSeTe/CdTe devices.

5. Conclusions

The effects of the $CdCl_2$ passivation treatment on the grain structure of CdSeTe/CdTe absorber and photovoltaic devices have been analyzed. The investigation presented here shows the effect of the $CdCl_2$ passivation treatment on sublimated CdSeTe/CdTe absorber films. Photovoltaic devices with a similar structure have been used to demonstrate a conversion efficiency of over 19% [6]. It is observed that prior to the $CdCl_2$ passivation treatment, the CdSeTe and CdTe grains contain a high density of stacking faults. The density of stacking faults in the CdSeTe grains appears to be higher than that observed in the CdTe grains. The $CdCl_2$ treatment is known to remove stacking faults in CdTe thin-films and we now have evidence that a similar effect occurs in CdSeTe films. After the $CdCl_2$ passivation treatment the stacking faults are completely removed in the CdSeTe and the CdTe layer. The stacking faults are tetrahedral and of such low energy that they will not act as recombination centers. However, we do observe a clear correlation between enhanced conversion efficiency and removal of these defects and this is probably associated with full passivation of the terminating grain boundaries. This work confirms that the $CdCl_2$ treatment is equally effective for defect passivation in CdSeTe/CdTe absorber thin-films. In addition to defect passivation, the $CdCl_2$ treatment also causes grain growth and recrystallization of the CdSeTe/CdTe films. Prior to the $CdCl_2$ passivation treatment, a large number of small CdSeTe grains are observed at the front interface with the MZO buffer layer. However, after the $CdCl_2$ passivation treatment substantial grain growth is observed. The CdSeTe grains appear to have merged to form larger grains by agglomeration.

Elemental distribution in the films has been investigated to observe diffusion caused by the $CdCl_2$ treatment. An abrupt interface between CdSeTe and CdTe layer is observed prior to $CdCl_2$ passivation treatment. After the $CdCl_2$ treatment, the CdSeTe and CdTe layers interdiffused with the movement of Se in the CdTe layer. CdSeTe and CdTe grains merge to form larger grains. This diffusion of Se leads to the formation of a CdSeTe/CdTe graded absorber layer and removes the abrupt interface between these layers. Surprisingly, the high temperature depositions and the $CdCl_2$ treatment do not cause depletion or diffusion of the MZO layer. The $CdCl_2$ passivation treatment is fortuitously effective as a process to cause CdSeTe/CdTe diffusion to create a graded layer in the device.

The electrical performance of a CdSeTe/CdTe absorber device is drastically improved after the $CdCl_2$ passivation treatment. The devices show improvement in J_{SC}, V_{OC} and fill-factor. The $CdCl_2$ treatment is equally effective as a defect passivation treatment for this new device

structure as it is for conventional thin film CdS/CdTe devices. Further optimization of this treatment will lead to improved device performance.

The $Mg_xZn_{1-x}O$ (x = 23) buffer used in device structure was optimized for higher band-gap CdTe absorber. CdTe graded with CdSeTe is used in these devices with CdSeTe forming and interface with MZO. Since CdSeTe has a lower band-gap as compared to CdTe, it would be important to again optimize the buffer layer for the lower band-gap. In addition, future work would include optimization of CdSeTe composition and grading to improve device efficiency.

Acknowledgements

Authors would like to thank everyone at Colorado State University's Next Generation Photovoltaics Center who, although not directly involved in this study, contributed to its success through experimental preparation and discussion—particularly Prof. James R. Sites. We are also thankful to Kevan Cameron and the undergraduate staff at CSU's Next Generation Photovoltaics Center for help with tool maintenance and device measurements. This work was partially supported by the National Science Foundation (NSF) Industry/University Collaborative Research Center (I/UCRC) under award number 1540007, National Science Foundation (NSF) PFI:AIR-RA program under award number 1538733 and U.S. Department of Energy (DOE) Small Innovative Projects in Solar (SIPS) under award number DE-EE0008177. The authors at Loughborough University are grateful to RCUK for funding through the EPSRC Supergen SuperSolar Hub (EP/J017361/1).

Appendix A. Supporting information

Supplementary data associated with this article can be found in the online version at http://dx.doi.org/10.1016/j.solmat.2018.06.016.

References

[1] N.M. Haegel, R. Margolis, T. Buonassisi, D. Feldman, A. Froitzheim, R. Garabedian, M. Green, S. Glunz, H.-M. Henning, B. Holder, I. Kaizuka, B. Kroposki, K. Matsubara, S. Niki, K. Sakurai, R.A. Schindler, W. Tumas, E.R. Weber, G. Wilson, M. Woodhouse, S. Kurtz, Terawatt-scale photovoltaics: trajectories and challenges, Sci. (80-.) 356 (6334) (2017).

[2] M.A. Green, Y. Hishikawa, W. Warta, E.D. Dunlop, D.H. Levi, J. Hohl-Ebinger, A.W.H. Ho-Baillie, Solar cell efficiency tables (version 50), Prog. Photovolt. Res. Appl. 25 (7) (2017) 668–676.

[3] W. Eric, Exclusive: first Solar's CTO Discusses Record 18.6% Efficient Thin-Film Module, Greentech Media, 2015 (Online). (Available), ⟨http://www.greentechmedia.com/articles/read/Exclusive-First-Solars-CTO-Discusses-Record-18.6-Efficient-Thin-Film-Mod⟩.

[4] S.K.David. Brady, Steve Haymore, First Solar, INC. Announces First Quarter 2014 Financial Results, Tempe, AZ, 2014.

[5] S.K.Steve. Haymore, First Solar, Inc., 2016 First Quarter Financial Results, Tempe, AZ, 2016.

[6] A. Munshi, J. Kephart, A. Abbas, J. Raguse, J. Beaudry, J. Sites, J. Walls, K. Barth, and W. S. Sampath. "Polycrystalline CdSeTe / CdTe Absorber Cells With," vol. 8, no. 1, 2018, pp. 310–314.

[7] A.H. Munshi, J.M. Kephart, A. Abbas, T.M. Shimpi, K.L. Barth, J.M. Walls, W.S. Sampath, Polycrystalline CdTe photovoltaics with efficiency over 18% through improved absorber passivation and current collection, Sol. Energy Mater. Sol. Cells 176 (2018) 9–18 (no. July 2017).

[8] Ali Abbas, Geoff D. West, Jake W. Bowers, Piotr M. Kaminski, John M. Walls, Kurt L. Bart, W.S. Sampath, Cadmium chloride assisted re-crystallisation of CdTe: the effect on the CdS window layer, MRS Proc. 1738 (2015).

[9] Geoff D. Ali Abbas, Jake W. West, Piotr M. Bowers, B. Kaminski, John M. Maniscalco, Kurt L. Walls, Barth, W.S. Sampath, Cadmium chloride assisted re-crystallization of CdTe: the effect of varying the annealing time, MRS Proc. 1638 (2014).

[10] C. Li, Y. Wu, J. Poplawsky, T.J. Pennycook, N. Paudel, W. Yin, S.J. Haigh, M.P. Oxley, A.R. Lupini, M. Al-Jassim, S.J. Pennycook, Y. Yan, Grain-boundary-enhanced carrier collection in CdTe solar cells, Phys. Rev. Lett. 112 (15) (2014) 156103.

[11] J.M. Kephart, Optimization of the Front Contact to Minimize Short-circuit Current Losses in CdTe Thin-film Solar Cells, Colorado State Univeristy, 2015.

[12] M. Kephart Jason, M. Geisthardt Russell, S. Sampath Walajabad, Optimization of CdTe thin-film solar cell efficiency using a sputtered, oxygenated CdS window layer, Prog. Photovolt. 23 (11) (2015) 1484–1492.

[13] D.E. Swanson, J.M. Kephart, P.S. Kobyakov, K. Walters, K.C. Cameron, K.L. Barth, W.S. Sampath, J. Drayton, J.R. Sites, Single vacuum chamber with multiple close space sublimation sources to fabricate CdTe solar cells, J. Vac. Sci. Technol. A Vac. Surf. Film. 34 (2) (2016) 21202.

[14] KurtL Barth, Sampath, S. Walajabad, R.A. Enzenroth, Apparatus and Processes for the Mass Production of Photovoltaic Modules, 2002.

[15] S. Yoo, K.T. Butler, A. Soon, A. Abbas, J.M. Walls, A. Walsh, Identification of critical stacking faults in thin-film CdTe solar cells, Appl. Phys. Lett. 105 (2014) 62104 (no. May).

[16] A. Munshi, Investigation of Processing, Microstructures and Efficiencies of Polycrystalline CdTe Photovoltaic Films and Devices, Colorado State Univeristy, 2016.

[17] A. Munshi, A. Abbas, J. Raguse, K. Barth, J.M. Walls, W.S. Sampath. Effect of varying process parameters on CdTe thin film device performance and its relationship to film microstructure, 2014, pp. 1643–1648.

[18] B.E. McCandless, Ã.L.V. Moulton, R.W. Birkmire, L.V. Moulton, R.W. Birkmire, Recrystallization and sulfur diffusion in CdCl2-treated CdTe/CdS thin films, Prog. Photovolt. Res. Appl. 5 (1997), pp. 249–260 (no. May).

[19] A. Abbas, D. Swanson, A. Munshi, K.L. Barth, W.S. Sampath, G.D. West, J.W. Bowers, P.M. Kaminski, and J.M. Walls, "The effect of a post-activation annealing treatment on thin film cdte device performance, in: Proceedings of the IEEE 42nd Photovoltaics Specialist Conference PVSC, 2015.